AUTOMATIC BRAIN TUMOR SEGMENTATION USING TISSUE DIFFISIVITY CHARACTERISTICS

Azadeh Yazdan-Shahmorad[1,2,3], Hesamoddin Jahanian[1,3], Suresh Patel[1], Hamid Soltanian-Zadeh[1,2,4]

[1]Medical Image Analysis Lab., Radiology Dept., Henry Ford Health System, Detroit, Michigan, USA
[2]Electrical and Computer Engineering Department, Wayne State University, Detroit, Michigan, USA
[3]Biomedical Engineering Department, University of Michigan, Ann Arbor, Michigan, USA
[4]Control and Intelligent Processing Center of Excellence, Elec. and Comp. Eng. Dept., Faculty of Engineering, University of Tehran, Tehran, Iran

ABSTRACT

Water diffusion measurements have been shown to be sensitive to tissue cellular size, extra cellular volume, and membrane permeability. Therefore, diffusion tensor imaging (DTI) by magnetic resonance imaging (MRI) can be used to characterize highly cellular regions of tumors versus acellular regions, distinguishing cystic regions from solid regions. An automatic segmentation method is proposed in this paper based on a multi-phase clustering algorithm to segment the brain tumors in a feature space extracted from DTI images. The algorithm is applied on DTI images of a total of 20 patients with 4 different types of tumors. The tumor region segmentation was 92% accurate based on the segmentation results using anatomical images and 100% accurate based on biopsy results. In general, the segmentation results obtained by the proposed method revealed a strong agreement with the biopsy results and anatomical images, providing support for the accuracy and robustness of the proposed feature space and the segmentation procedure.

Index terms: diffusion tensor imaging (DTI), magnetic resonance imaging (MRI), segmentation, water diffusivity, tumor.

1. INTRODUCTION

An important step in image analysis is to associate with each image pixel a particular tissue class based on the pixel's attributes which is called tissue segmentation [1]. Exact brain tumor segmentation plays a significant role in the treatment of malignant tumors [2].

Manually segmenting brain tissues is generally time-consuming, irreproducible, and difficult. In most settings, the task is performed by marking the tumor regions slice-by-slice, which limits the human rater's view and generates jaggy images [2]. An accurate, reproducible, and automated segmentation method is desirable to reduce the misclassification error and generate satisfactorily reproducible segmentation results.

The use of water diffusion as a surrogate marker to probe tissue cellularity is compelling because this parameter is strongly affected by molecular viscosity and membrane permeability between intra-and extracellular compartments, active transport and flow, and directionality of tissue/cellular structures that impede water mobility [3]. For example, water diffusion measurements have been shown to be sensitive to tissue cellular size, extra cellular volume, and membrane permeability [4]. Therefore, diffusion tensor imaging (DTI) by magnetic resonance imaging (MRI) can be used to characterize highly cellular regions of tumors versus acellular regions, distinguishing cystic regions from solid regions, as well as detection of treatment response, which is manifested as a change in cellularity within the tumor over time [3].

Structurally anisotropic tissues, such as white matter, can exhibit persistent diffusion anisotropy, despite a diffusion coefficient elevated by edema. This could potentially provide contrast between edema and anisotropic solid tumor [4] and can be used for accurate tumor segmentation. In the present study, considering the diffusion characteristics of tumor and its surrounding edema, an algorithm is proposed to automatically segment the tumor region and specifically distinguish it from edema.

2. MATERIALS AND METHODS

2.1. DTI Data

DTI images of a total of 21 patients with 4 different types of tumors were acquired (8 patients with Glioma, 5 patients with Oligodendroglioma, 7 patients with Astrocytoma, and 1 patient with Oligoastrocytoma).

Diffusion weighted images were acquired using a 3T GE Signa MRI scanner (General Electric, Milwaukee, WI). Patients were scanned using 25 noncollinear weighting directions and a single shot echo planar imaging (EPI) sequence with TR/TE = 10000/71.8 ms and b value of 1000

sec/mm2 and one additional b=0 image. Each volume covers a 240 mm x 240 mm field of view with 0.9375 mm x 0.9375 mm in-plane resolution and 5 mm slice thickness and no gap between slices.

2.2. Proposed Feature Space

The proposed feature space consists of two categories: DTI features which introduce the diffusivity characteristics to the feature space and spatial features which correspond to the spatial information (connectivity) of tissues.

Once the diffusion tensor is calculated, a range of quantities can be easily derived which will be discussed. To obtain an overall evaluation of the diffusion in a voxel or region, one must avoid anisotropic diffusion effects and limit the result to an invariant, i.e., a quantity that is independent of the orientation of the reference frame [5]. Among several combinations of the tensor elements, the trace of the diffusion tensor, which is calculated using the following equation is such an invariant [6].

$$T_r(D) = D_{xx} + D_{yy} + D_{zz} \quad (1)$$

The diffusion tensor may be conveniently visualized by a diffusion ellipsoid. The three principal axes of the ellipsoid correspond to the three eigenvectors of the diffusion tensor [7]. The eigenvalues λ_1, λ_2 and λ_3, which correspond to the three eigenvectors, represent the magnitude of diffusivity in the three directions. Based on these three diffusivities and the mean diffusivity (λ), the fractional anisotropy (FA) can be calculated to yield values between 0 and 1:

$$FA = \frac{\sqrt{3}}{\sqrt{2}} \frac{\sqrt{(\lambda_1 - \lambda)^2 + (\lambda_2 - \lambda)^2 + (\lambda_3 - \lambda)^2}}{\sqrt{\lambda_1^2 + \lambda_2^2 + \lambda_3^2}} \quad (2)$$

where

$$\lambda = \frac{\lambda_1 + \lambda_2 + \lambda_3}{3} \quad (3)$$

Two other commonly used anisotropy definitions are the relative anisotropy (RA) and the volume ratio (VR), defined, respectively, as [7]:

$$RA = \frac{\sqrt{3}}{\sqrt{2}} \frac{\sqrt{(\lambda_1 - \lambda)^2 + (\lambda_2 - \lambda)^2 + (\lambda_3 - \lambda)^2}}{\lambda_1 + \lambda_2 + \lambda_3} \quad (4)$$

$$VR = 1 - \frac{\lambda_1 \lambda_2 \lambda_3}{\lambda^3} \quad (5)$$

As there have been reports on changes of the described indices inside the tumor with respect to normal tissues in the literature[1,2,3,4,7], the following features have been computed: mean of apparent diffusion coefficient (ADC) [6] values, standard deviation of ADC values, tensor values: D_{xx} , D_{yy} , D_{zz} , D_{xy} , D_{xz} , D_{yz}, tensor trace , eigenvalues, and FA, RA, and VR values.

As the exact region of the brain tumor in patients is unknown, we had to apply several evaluation methods to select the best feature set. The first method used in feature selection phase was Sequential Backward Selection (SBS) [8]. The evaluation in this method was done by a clinical expert based on the available anatomical images. In order to have the best evaluation, the proposed algorithm was applied to 10 patients with different tumor types. The best results were achieved with the following set of features: ADC mean, eigenvalues, tensor trace, FA, and VR values.

The algorithm did not perform well in the presence of ADC standard deviation (std) feature and the results were not changed by adding or removing tensor values in almost all of the studied patients. While we had FA value in the examined feature space, presence of RA value had no effects on the results. In this step, the ADC std and RA features were eliminated and the other features were examined by the following method.

In this method, the evaluation was performed on inter-class and intra-class distance distributions. Using the Euclidean distance measure for each of the features, we generated the inter-class and intra-class distance distributions for the segmented regions from images of the 10 patients.

The overlapping area between the inter-class and intra-class distributions was calculated for each feature. The average of the overlapped area for each feature using the calculated overlapped areas of all patients show that the tensor values: D_{xx} , D_{yy} , D_{zz} , D_{xy} , D_{xz} , D_{yz} and the second and third eigenvalues (λ_2 , λ_3) have more than 35 percent overlap in their distributions and in comparison to other features can reduce the classification accuracy. Therefore, these features are eliminated from the extracted features and the final features are: ADC mean, the largest eigenvalue: λ_1, tensor trace, FA, and VR values.

To take our prior knowledge about the spatial distribution (connectivity) of tumor tissues into account, spatial features need to be added to the DTI feature space. A naive approach for introducing spatial information to our clustering algorithm was to add the coordinates of each pixel as features to the clustering algorithm [9]. This approach helped to discriminate between tissue segments with overlapping ranges of other features, and to suppress noise effects.

2.3. Classification

The brain tumor segmentation method is done in three classification phases. Each step uses the k-means clustering algorithm. The distance metric used in the present study is the Euclidean distance.

The first phase deals with the separation of background from the brain pixels. In this phase, the extracted features are classified into two clusters, one for each background and brain. At the end of this stage, a binary image specifying 1 to brain and 0 to background pixels is generated.

In the second phase, the normal brain is separated from other pixels inside the brain. The k-means algorithm is applied to the brain pixels separated in the previous phase. The number of clusters is set to 3. Since even the largest

tumors in the available data set are about the 20 percent of the whole brain, the cluster with the largest number of pixels in this step is related to a large portion of brain with normal tissues. It is advantageous to remove these pixels from the selected set, because the differences between the tumor region and the area around it that may be edema can be better realized by the classifier in the third phase.

In this last phase, the k-means clustering with two clusters is applied. The number of clusters in this step is set to two for the brain and tumor tissues.

2.4. Post Processing

Brain tumors are difficult to segment because they have a wide range of appearance and effect on surrounding structures. In addition, there are several distortions that may affect the segmentation results. To overcome these problems, the following post processing methods are applied to the segmented images.

Due to low SNR of DTI images, a lot of small objects in the brain may be classified in the same cluster with the tumor pixels. To overcome this problem, an area thresholding algorithm has been applied to the segmented connected components.

In addition to the small noisy objects, large noisy connected components may appear in the segmented image in the same cluster with the tumor region. Our assumption is that the tumor appears as a connected component which has a shape of a circle or an ellipse in general. But the noisy objects do not have a particular shape and usually appear in different noisy patterns. Two shape parameters (aspect ratio and solidity) are used to detect these objects and remove them from the segmentation results.

3. EXPERIMENTAL RESULTS

To evaluate the proposed algorithm, the segmentation results are compared with those of the Eigen segmentation [10]. This method segments the image based on FLAIR, T2, T1-pre and T1-post contrast images of the brain. The comparisons based on applying the two segmentation methods to diffusion tensor and anatomical images of the 10 test patients are shown in Table 1.

The results show 100 percent accuracy for the proposed method, using DTI feature space, based on the biopsy points. In comparison to the corresponding results of Eigen segmentation, we can conclude that the proposed algorithm can distinguish tumor from edema using the mentioned features extracted from DTI. In addition, the accuracy percentage reported in Table 1 shows that the DTI extracted features contain more information about the tumor characteristics in comparison to the anatomical images. Figure 1A shows the segmentation results of the proposed method and Figure 1B-C show the corresponding anatomical images. While the tumor region shown in the anatomical images is small, tumor tissues are diagnosed in all of the biopsy points (Figure 1D-F), which shows the existence of tumor in all of the suspected regions. As seen in Figure 1A, the proposed algorithm has segmented the tumor region correctly based on the biopsy results.

In general, the brain tumor segmentation method used in this study showed strong agreement with the anatomical images and biopsy results, providing support for the accuracy and robustness of the features and the segmentation procedure used.

4. DISSCUSSION

To the mentioned advantages of the proposed tumor segmentation algorithm in comparison to the common methods, the significant reduction in image acquisition time should be added. The approximate acquisition time for diffusion tensor imaging is about 5 minutes while the acquisition time for T1, T2, and FLAIR images is about 25 minutes. This time reduction benefits both patients and physicians. In addition, there is no need for the injection of contrast agents in DTI. The two latter described advantages will also reduce the cost of tumor diagnosis.

Table 1. Comparison of the Eigen segmentation with the presented method based on biopsy results, TD: Tumor Diagnosed, BD: Brain Diagnosed, CD: Correct Diagnosed

Patient No.	No. of Biopsy Points	Pathology Results		Eigen segmentation						Proposed Method					
				Anatomical Images			DTI Feature Space			Anatomical Images			DTI Feature Space		
		TD Points #	BD Points #	TD Points #	BD Points #	CD %	TD Points #	BD Points #	CD %	TD Points #	BD Points #	CD %	TD Points #	BD Points #	CD %
5	7	7	0	7	0	100	6	1	85	7	0	100	7	0	100
6	2	2	0	2	0	100	2	0	100	2	0	100	2	0	100
7	3	2	1	3	0	66	3	0	66	3	0	66	2	1	100
8	5	4	1	4	1	100	3	2	80	4	1	100	4	1	100
11	4	4	0	4	0	100	4	0	100	3	1	75	4	0	100
12	11	11	0	11	0	100	8	3	72	7	4	63	11	0	100
13	17	14	3	15	2	94	15	2	94	13	4	94	14	3	100
17	6	4	2	4	2	100	6	0	66	6	0	66	4	2	100
18	6	4	2	6	0	66	5	1	83	6	0	66	4	2	100
19	6	5	1	6	0	83	6	0	83	6	0	83	5	1	100
Average						90.9			82.9			81.3			100

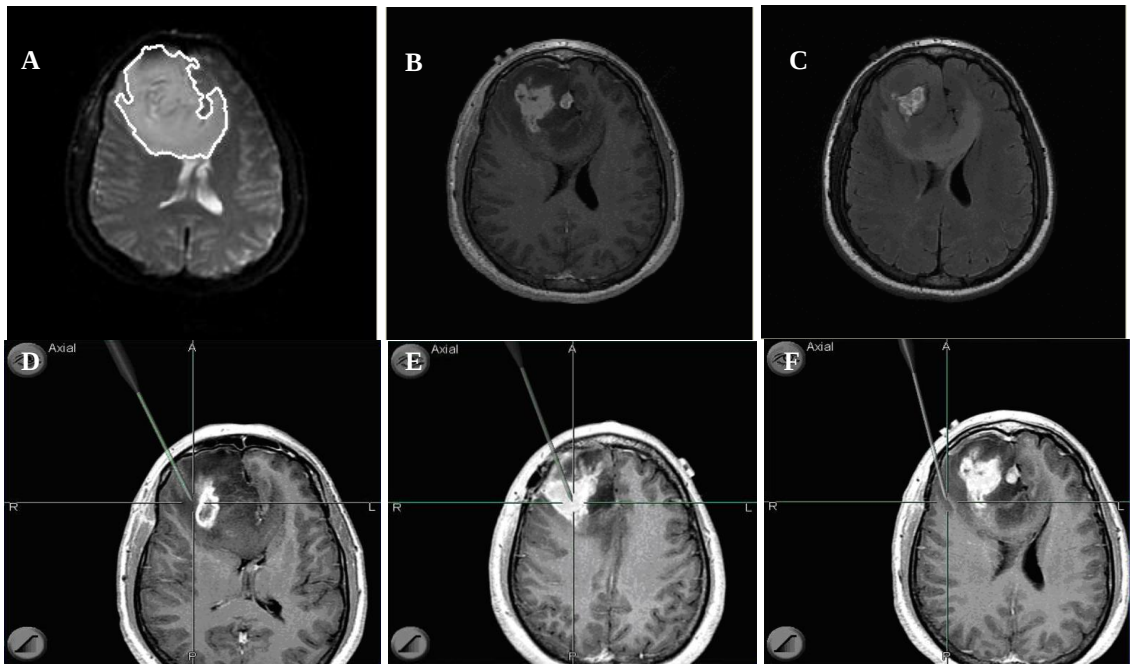

Figure 1. A: segmentation results of the proposed method, **B:**T1 post contrast image, **C:** FLAIR image, **D-F:** Biopsy points. While the tumor region shown in the anatomical images is small, tumor tissues were diagnosed in all of the biopsy points, which shows the existence of tumor in all of the suspected regions. As seen in A, the proposed algorithm has segmented the tumor region correctly (based on the biopsy results).

5. CONCLUSION

This study proposed a three-dimensional brain tumor segmentation algorithm based on the diffusivity characteristics of the tissues. The results indicate that based on the differences of the extracted features from diffusion tensor images in tumor and brain tissues, not only tumor region can be segmented but it also can be differentiated from its surrounding edema. The consistency of the segmentation results in the present study with the biopsy results provides support for the accuracy and robustness of the features and the segmentation procedure. Considering the image acquisition time of DTI in comparison to other MRI techniques such as T1, T2, and FLAIR, this algorithm can replace the common tumor segmentation methods in clinical applications.

6. REFERENCES

[1] A. Hadjiprocopis,W. RashidT and P.S. Tofts "Unbiased segmentation of diffusion-weighted magnetic resonance images of the brain using iterative clustering," *Magnetic Resonance Imaging* ,Vol.23, pp. 877–885, 2005.

[2] K. Xiea, J. Yanga, Z.G. Zhanga and Y.M. Zhuba "Semi-automated brain tumor and edema segmentation using MRI," *European Journal of Radiology*,Vol.56, pp.12–19, 2005.

[3] B.D. Ross, B.A. Moffat, T.S. Lawrence, S. K. Mukherji, S.S. Gebarski, D.J. Quint, T.D. Johnson, L. Junck, P.L. Robertson, K.M. Muraszko, Q. Dong, C.R. Meyer, P.H. Bland, P. McConville, H. Geng, A. Rehemtulla and T.L. Chenevert "Evaluation of cancer therapy Using Diffusion Magnetic Resonance Imaging," *Molecular Cancer Therapeutics*, Vol.2, pp.581–587, June 2003.

[4] T.L. Chenevert, P.E. McKeever and B.D. Ross "Monitoring early response of experimental brain tumors to therapy using Diffusion Magnetic Resonance Imaging," *Clinical Cancer Research*, Vol.3, pp.1457-1466, September 1997.

[5] P.J. Basser, J. Mattiello and D. Le Bihan "MR diffusion tensor spectroscopy and imaging,". *Biophysics Journal*, Vol.66, pp.259–267, 1994.

[6] D. L. Bihan, J. F. Mangin, C. Poupon, C.A. Clark, S. Pappata, N. Molko and H. Chabriat, "Diffusion Tensor Imaging: Concepts and Applications," *Joural of Magnetic Resonance Imaging*, Vol.13, pp.534–546, 2001.

[7] C. Pierpaoli and P.J. Basser, "Toward a quantitative assessment of diffusion anisotropy," *Magnetic Resonance in Medicine*, Vol. 36, pp.893–906, 1996.

[8] E. Cantu-Paz, S. Newsam and C. Kamath, , "Feature Selection in Scientific Applications," *Proceedings of International Conference on Knowledge Discovery and Data Mining*, Seattle,WA, pp.788-793, August 22-25, 2004.

[9] Jain, R., R. Kasturi and B.G. Schunck, *Machine Vision*, McGraw-Hill, NewYork, NY, USA, 1995.

[10] H. Soltanian-Zadeh, D.J. Peck, J.P. Windham and T. Mikkelsen,"Brain tumor segmentation and characterization by pattern analysis of multispectral NMR images," *NMR in Biomedicine*, Vol.11, Issue.4-5, pp.201-8, 1998.